Impacts of initial conditions on monsoon intraseasonal forecasting

Xiouhua Fu,[1] Bin Wang,[1,2] Qing Bao,[3] Ping Liu,[1] and June-Yi Lee[1]

Received 6 January 2009; revised 3 March 2009; accepted 19 March 2009; published 16 April 2009.

[1] Sensitivity of monsoon intraseasonal forecasting to different initial conditions is examined with the University of Hawaii Hybrid Coupled Model (UH_HCM). The target period is May to September 2004. We found that in the NCEP reanalysis the amplitudes of the convective activities associated with monsoon intraseasonal oscillation (MISO) are smaller than the observed counterparts by a factor of two to three. Motivated by this fact, we carried out a suite of forecasting experiments to explore the impacts of initial conditions on intraseasonal forecast skills. Our results reveal that with the original NCEP reanalysis as initial conditions the monsoon intraseasonal forecast skills of 850-hPa zonal winds and rainfall are only about a week over the global tropics (30°S–30°N) and Southeast Asia (10°N–30°N, 60°E–120°E). The predictability increases steadily with increased amplitudes of MISO in the initial conditions. When the MISO signals in initial conditions are recovered to a level similar to that in the observations, monsoon intraseasonal forecast skills reach 25 days for 850-hPa zonal winds and 15 days for rainfall over both the global tropics and Southeast Asia. It is also found that high-frequency weather in initial conditions generally extends rainfall predictability by about 5 days. **Citation:** Fu, X., B. Wang, Q. Bao, P. Liu, and J.-Y. Lee (2009), Impacts of initial conditions on monsoon intraseasonal forecasting, *Geophys. Res. Lett.*, *36*, L08801, doi:10.1029/2009GL037166.

1. Introduction

[2] Monsoon Intra-Seasonal Oscillation (MISO) with 30- to 90-day period is a fundamental building block of summer monsoon. The MISO influences the onset, retreat and wet/dry phases of monsoon [*Yasunari*, 1979]. The active phase of MISO also modulates the genesis/intensification of tropical cyclones [e.g., *Maloney and Hartmann*, 2000; *Wang and Zhou*, 2008]. The MISO originates in the western tropical Indian Ocean and propagates northeastward to Southeast Asia and the Western North Pacific (WNP) [e.g., *Wang et al.*, 2006]. It also propagates eastward along the equatorial Pacific and is amplified over the Eastern North Pacific [*Maloney and Esbensen*, 2003], where it propagates northward to significantly influence the North American summer monsoon [*Jiang and Waliser*, 2008]. The capability of forecasting monsoon intraseasonal oscillation beyond two weeks is extremely desirable and has great benefits for the inhabitants of monsoon regions. The present study is a step towards this goal by expanding our understanding of the impacts of initial conditions.

[3] Due to the chaotic nature of Earth's atmosphere, numerical weather prediction is very sensitive to atmospheric initial conditions [*Lorenz*, 1993]. On the other hand, seasonal forecasts (largely based on ENSO) are primarily determined by sea surface temperature anomaly [*Shukla*, 1998]. For an intraseasonal variability with a time scale between synoptic weather and seasonal climate, the predictability of MISO is sensitive to both atmospheric initial conditions and lower boundary conditions [*Waliser et al.*, 2003; *Fu et al.*, 2007]. The recent study of *Fu et al.* [2008a] further demonstrated that, in order to allow the underlying SST anomaly to extend the MISO potential predictability, the atmospheric initial conditions must be sufficiently accurate. The possible impact of under-represented intraseasonal variability in initial conditions on the practical predictability of MISO will be investigated in this study.

[4] Many previous studies on ISO forecasting [e.g., *Hendon et al.*, 2000; *Vitart et al.*, 2007; *Fu et al.*, 2008b] have commonly used two reanalysis datasets (NCEP and ECMWF) as atmospheric initial conditions. One of our concerns is the accuracy of the initial conditions. From an observational point of view, the strongest convective signals of ISO exist in the equatorial Indian and western Pacific Oceans [*Wang et al.*, 2006], where only very sparse in-situ observations are available. Over these oceanic regions, the quality of reanalysis datasets largely depends on the physics of individual models that were used for data assimilation. It is well-known that most contemporary global models considerably underestimate ISO variability [*Lin et al.*, 2006]. These limitations suggest that the intraseasonal variability in current reanalysis datasets may be underestimated. *Shinoda et al.* [1999] found that the convective activities associated with ISO in the NCEP reanalysis are smaller by a factor of 2 to 3 than that in the observations during 1982–1989. Furthermore, the experimental forecasts conducted by *Krishnamurti et al.* [1992] have used a special procedure to generate atmospheric initial conditions, in which only time-mean and intraseasonal variability are included. It is unknown how this initial filtering of the weather component impacts the MISO forecast skill.

[5] In the present study, the impacts of including/excluding weather activities in initial conditions [e.g., *Krishnamurti et al.*, 1992] on MISO forecasting will be assessed. Moreover, we will explore various ways to modify the strength of the intraseasonal variability in the NCEP reanalysis and examine how the modified initial conditions will impact MISO forecast skills. The model used in this study and the experimental designs are described in section 2, followed by sensitivity experiment results. In section 4, we

[1] IPRC, SOEST, University of Hawaii at Manoa, Honolulu, Hawaii, USA.
[2] Department of Meteorology, SOEST, University of Hawaii at Manoa, Honolulu, Hawaii, USA.
[3] LASG, Institute of Atmospheric Physics, Chinese Academy of Sciences, Beijing, China.

0094-8276/09/2009GL037166$05.00

Table 1. Five Different Initial Conditions Used for MISO Forecasting Experiments

EXP	Initial Conditions[a]
NCEP_R_f	AC[b] + filtered[c]
NCEP_R_unf	AC + filtered + high-frequency[d]
2*NCEP_R_f	AC + 2*filtered
3*NCEP_R_f	AC + 3*filtered
3*NCEP_R_unf	AC + 3*filtered + high-frequency

[a]The procedure used to generate initial conditions is briefly given here: First, the NCEP reanalysis data from January 1 to December 31, 2004 were decomposed into an annual cycle (annual mean plus first three annual harmonics), 30–90-day variability, and high-frequency variability with a Fourier transform. For the first filtered experiment (i.e., NCEP_R_f), only the annual cycle and 30–90-day variability are combined and interpolated onto UH_HCM model grids. To minimize the initial shock, the interpolated PBL temperature and pressure have been adjusted to satisfy a hydrostatic equation. The interpolated data, then, were nudged into the UH_HCM model to generate initial conditions.
[b]AC (Annual Cycle) = Annual mean + First three annual harmonics.
[c]Filtered = 30–90-day variability.
[d]High-frequency = Total – AC – filtered.

summarize our chief findings and discuss possible future studies.

2. Model and Experimental Designs

[6] The model used to carry out experimental MISO forecasting is the University of Hawaii Hybrid Coupled Model (UH_HCM), which comprises ECHAM-4 AGCM with an intermediate ocean model. The UH_HCM can simulate Asian summer monsoon and the associated intraseasonal oscillation reasonably well [*Fu et al.*, 2003; *Fu and Wang*, 2004]. The potential predictability of MISO in the UH_HCM reaches about 40 days over Southeast Asia [*Fu et al.*, 2008a]. In order to explore the impacts of initial ISO amplitudes and high-frequency weather on MISO forecast skills, five forecasting experiments were conducted by modifying the ISO amplitudes and by including/excluding high-frequency weather in initial conditions. The details of the experiments are given in Table 1.

[7] Summer of 2004 was selected as the target season. Under each initial condition (Table 1), ten ensemble forecasts are initiated from May 1st to October 1st in about 10-day interval. The ensemble initial conditions are generated by adding day-to-day differences of four prognostic variables (u, v, T, q) onto the unperturbed initial conditions [*Waliser et al.*, 2003]. In total, 16 two-month long forecasts (160 ensembles) were conducted under each setting of the five different types of initial conditions (Table 1). In the following analysis, only 10 ensemble means are analyzed.

3. Results

3.1. MISO Activity Is Underestimated in NCEP Reanalysis

[8] *Shinoda et al.* [1999] found that NCEP reanalysis significantly underestimates the ISO convective activities. *Fu and Wang* [2004] and *Fu et al.* [2006] found that the ISO-related moisture perturbations were significantly underestimated by ECMWF analysis in 1991–2000. *Tian et al.* [2006] also revealed that ISO-related humidity perturbations in NCEP reanalysis are underestimated, particularly over the Indian Ocean.

[9] To further examine to what degree MISO-related convection is underestimated by NCEP reanalysis, specifically during 2004 summer, a limited-domain wavenumber-frequency analysis [*Fu et al.*, 2003] has been applied to the daily rainfall in 2004 summer for two observational datasets (TRMM 3B42 and GPCP) and NCEP reanalysis. The resultant spectra associated with eastward-propagating rainfall are shown in Figure 1. The MISO-related rainfall variance in the observations is greater by a factor of 4 than that in the NCEP reanalysis. This result reveals that the MISO amplitude in the NCEP reanalysis during 2004 summer is still smaller by a factor of 2–3 than that in the observations, very similar to the case from two decades ago [*Shinoda et al.*, 1999].

3.2. Influence of Initial Conditions on Intraseasonal Forecasting

[10] The intraseasonal forecast skill is measured with an Anomaly Correlation Coefficient (ACC) [*Fu et al.*, 2007] over the global tropics (30°S–30°N) and Southeast Asia (10°N–30°N, 60°E–120°E). Before calculating the ACC, the observations (NCEP reanalysis 850-hPa zonal winds and GPCP rainfall) and the model ensemble-mean forecasts were filtered to retain only intraseasonal variability (30–90-day). (In order to extract intraseasonal variability from the forecasts, the observations from January 1, 2004 to the forecast starting times have been added to the two-months'

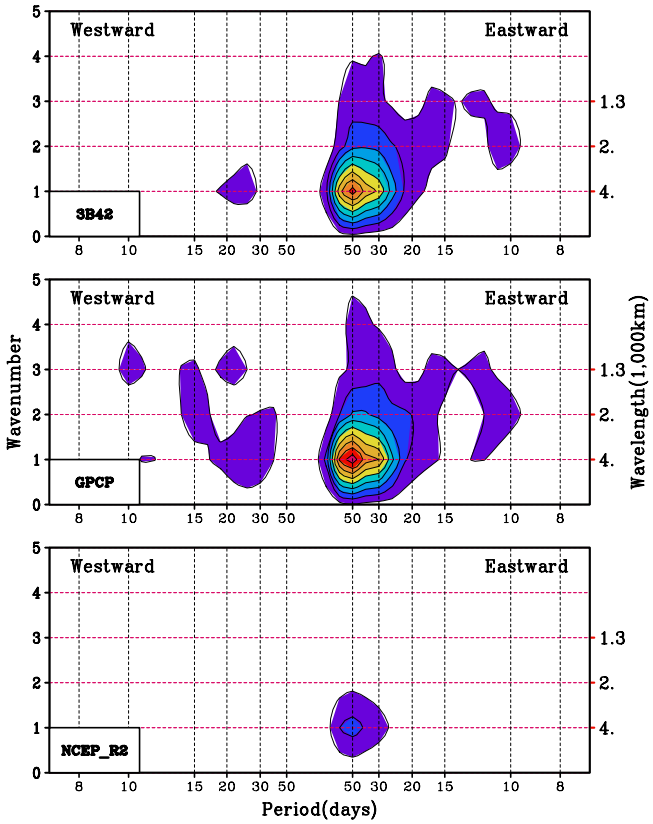

Figure 1. Wavenumber-frequency spectra of rainfall from TRMM 3B42, GPCP, and NCEP reanalysis averaged between 10°S and 10°N for zonally propagating disturbances in 2004 summer (MJJASO); Contours start from 2 with an interval of 2 (mm day^{-1})^2.

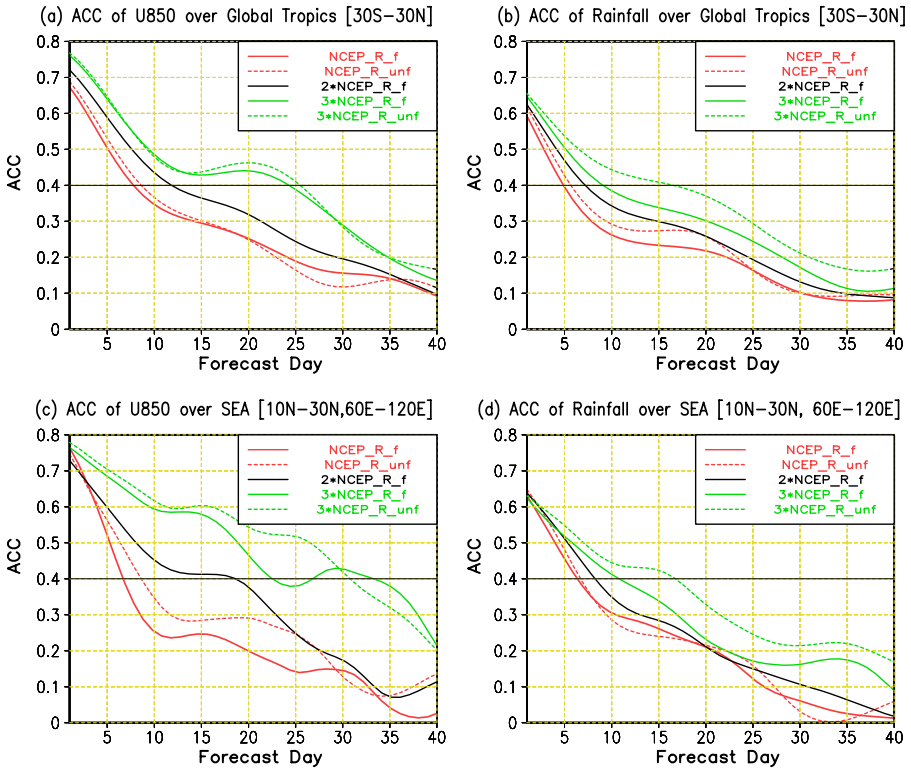

Figure 2. MISO forecast skills under different initial conditions (Table 1): (a) ACC of 30–90-day filtered 850-hPa zonal wind anomaly over the global tropics between 30°S and 30°N; (b) ACC of 30–90-day filtered rainfall anomaly over the global tropics; (c) ACC of 30–90-day filtered zonal wind anomaly over Southeast Asia (10°N–30°N, 60°E–120°E); and (d) ACC of 30–90-day filtered rainfall anomaly over Southeast Asia. To calculate the ACC of model forecasts, the zonal winds (rainfall) of NCEP reanalysis (GPCP) are used as the observations.

forecasts, followed by a smoothed annual cycle for the remaining days (annual mean plus first three annual harmonics of 2004) to create a 365-day time series. Then, a Fourier transform is applied to extract the 30–90-day variability.) The averaged ACC of 16 forecasts with a specific initial condition (Table 1) was plotted as a function of forecast lead time in Figure 2.

[11] A moderate value of ACC (0.4) was used to measure MISO practical predictability in days. The usefulness of this criterion was also illustrated by *Fu et al.* [2007, Figure 3]. When the high-frequency weather of the NCEP reanalysis is excluded from the initial condition (NCEP_R_f, Table 1), the predictability of U850 (rainfall) is about 7-day (5-day) over the global tropics (Figures 2a and 2b), and similar predictability is obtained for Southeast Asia (Figures 2c and 2d). Including high-frequency weather in the initial condition (NCEP_R_unf) does not degrade the overall forecast skill; rather it increases the forecast skill of U850 in Southeast Asia by 2–3 days (Figure 2c).

[12] When the MISO signals of NCEP reanalysis are doubled in the initial condition (2*NCEP_R_f), the intraseasonal forecast skills increase by about 5–10 days for U850 (Figures 2a and 2c) and about 2–3 days for rainfall (Figures 2b and 2d). When the MISO signals of NCEP reanalysis are tripled in the initial condition (3*NCEP_R_f), the intraseasonal forecast skill of U850 (rainfall) extends to about 25 days (10 days) over the global tropics and Southeast Asia. It is interesting to note that *including high-frequency weather in the initial condition (3*NCEP_R_unf) significantly extends rainfall predictability to more than 15 days* (Figures 2b and 2d). Obviously, inclusion of the multi-scale structure in the initial conditions has a positive contribution to MISO forecast, suggesting that adequate resolving of the high-frequency structure associated with the MISO in the initialization is necessary.

[13] The above results clearly demonstrate that when the MISO signals in the original NCEP reanalysis are "recovered" to a realistic level in the initial conditions (3*NCEP_R_unf), MISO practical predictability markedly increases compared to the results obtained by direct use of the original NCEP reanalysis as initial conditions (NCEP_R_unf). One example is given here to illustrate the impacts of different initial conditions on MISO forecasting. Figure 3 shows the initial intraseasonal rainfall anomalies from GPCP observations and three different experiments (NCEP_R_f, 2*NCEP_R_f, and 3*NCEP_R_unf, in Table 1) on May 31, 2004. The observations (GPCP, Figure 3a) show a tilted convective rainbelt extending from the southern tip of India, along the Indonesian island chain toward the northern tip of Australia. This tilted rainbelt is very weak in the filtered original NCEP reanalysis (NCEP_R_f, Figure 3b) but shows some intensification when MISO signals are doubled (2*NCEP_R_f, Figure 3c). When the MISO signals in the original NCEP reanalysis are tripled, the resultant initial rainfall anomaly (3*NCEP_R_unf, Figure 3d) becomes very similar to the observations; even the tilted convective rainbelt occurs over the south western Pacific. After 20 days, the observed active rainbelt has moved to the Bay of

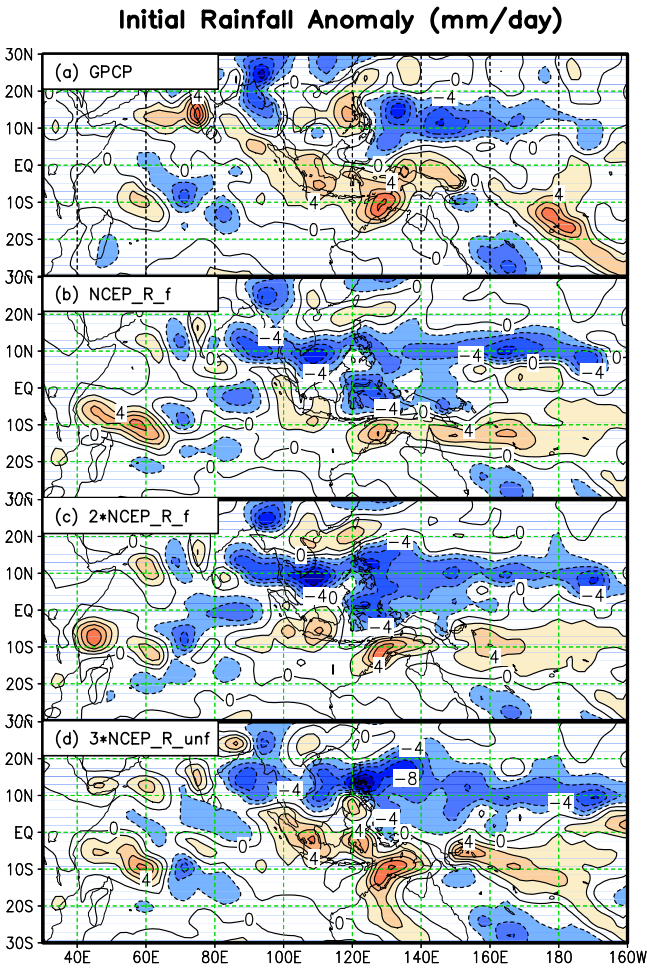

Figure 3. The 30–90-day filtered rainfall anomalies on May 31, 2004 from (a) the observations and different initial conditions: (b) NCEP_R_f, (c) 2*NCEP_R_f, and (d) 3*NCEP_R_unf. The initial conditions of the three experiments are found in Table 1.

Bengal and the WNP with an associated negative rainbelt to the south of it (Figure 4a). The forecasted rainfall anomaly, initiated with the filtered original NCEP reanalysis (NCEP_R_f, Figure 4b), is almost opposite to the observations: a negative rainfall anomaly over the Bay of Bengal and the WNP. When the initial MISO signals are doubled, some positive rainfall anomalies are forecasted in the WNP (2*NCEP_R_f, Figure 4c). However, the overall rainfall spatial pattern in the Indo-western Pacific region is still quite different from the observations. When the initial rainfall anomaly recovers to a level similar to the observations (Figure 3d), the resultant 20-day forecast (3*NCEP_R_unf, Figure 4d) also becomes similar to the observations (Figure 4a) with an active rainbelt over the Bay of Bengal and the WNP, along with a negative rainbelt to the south of it.

4. Concluding Remarks

[14] An atmosphere-ocean coupled model (UH_HCM) [*Fu and Wang*, 2004] has been used to examine the sensitivity of MISO forecast skills to different initial conditions (Table 1). First, a wavenumber-frequency analysis of 2004-summer rainfall reveals that the MISO convective activities in the NCEP reanalysis are smaller by a factor of 2 to 3 than that in the observations (Figure 1). When initial MISO amplitudes in the NCEP reanalysis gradually recover to the observed level (Figure 3), the forecast skills also steadily improve (Figures 2 and 4). The seasonal-averaged predictability of U850 (rainfall) reaches about 25 (15) days in the global tropics and Southeast Asia. It is also worth noting that the high-frequency variability (with period shorter than 30 days) in initial conditions does not decrease the overall forecast skill; rather, it extends the rainfall predictability by about 5 days (Figure 2). The underlying physics is a future research topic, particularly the individual contributions from variability less than 10 days and from that of 10–30 days.

[15] This study uncovers a drawback of using the NCEP reanalysis as initial conditions for intraseasonal forecasting. We propose a simple method to "recover" the intensity of the ISO activities in the reanalysis. The improved initial conditions show notably positive impacts on the monsoon intraseasonal forecast skills (Figures 2–4). Although many

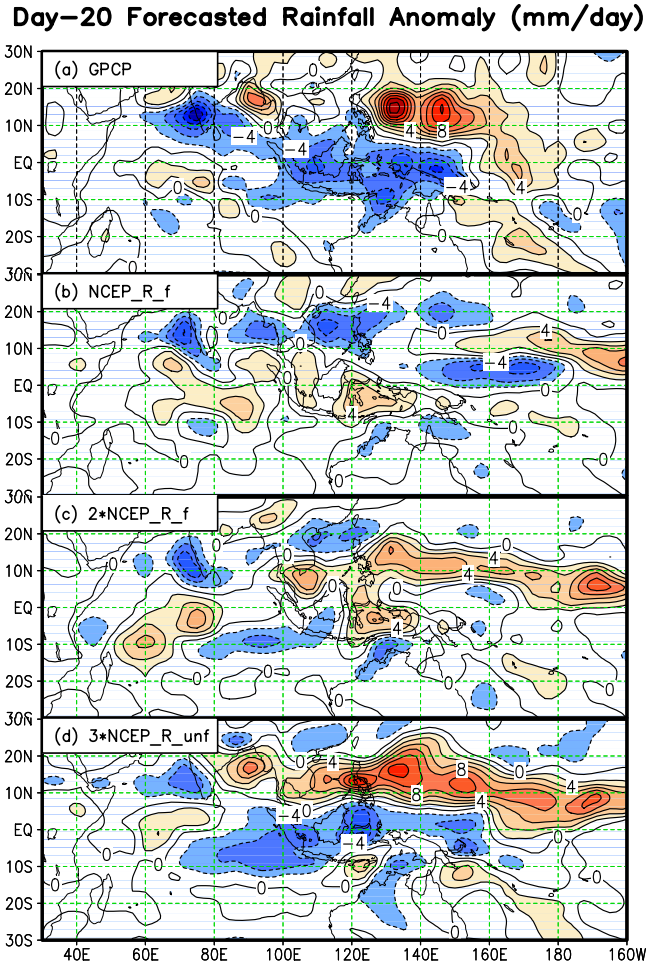

Figure 4. The 30–90-day filtered rainfall anomalies on June 20, 2004 from (a) the observations and different initial conditions: (b) NCEP_R_f, (c) 2*NCEP_R_f, and (d) 3*NCEP_R_unf. The initial conditions of three experiments are found in Table 1.

contemporary general circulation models still cannot realistically simulate ISO [*Lin et al.*, 2006], some models do show promise to forecast ISO beyond two weeks with useful skill [e.g., *Fu et al.*, 2008b; *Bechtold et al.*, 2008]. The potential socio-economic benefits from intraseasonal forecasting and preliminary results of the present study warrant that more dynamical forecasting experiments with different models and longer target periods should be conducted to better understand the impacts of initial conditions on intraseasonal forecasting and more studies are needed to develop methods that can generate better initial conditions for intraseasonal forecasting.

[16] **Acknowledgments.** This work was supported by NSF Climate Dynamics Program and by the Japan Agency for Marine-Earth Science and Technology (JAMSTEC), NASA, and NOAA through their sponsorship of the IPRC. BW and JYL are also supported by APEC Climate Center (APCC) as a part of APCC international research project. BQ is supported by 973 Program of China (2006CB403607). This paper is SOEST contribution 7671 and IPRC contribution 603.

References

Bechtold, P., M. Kohler, T. Jung, F. Doblas-Reyes, M. Leutbecher, M. J. Rodwell, F. Vitart, and G. Balsamo (2008), Advances in simulating atmospheric variability with the ECMWF model: From synoptic to decadal time-scales, *Q. J. R. Meteorol. Soc.*, *134*, 1337–1351.

Fu, X., and B. Wang (2004), The boreal-summer intraseasonal oscillations simulated in a hybrid coupled atmosphere-ocean model, *Mon. Weather Rev.*, *132*, 2628–2649.

Fu, X., B. Wang, T. Li, and J. P. McCreary (2003), Coupling between northward-propagating intraseasonal oscillations and sea surface temperature in the Indian Ocean, *J. Atmos. Sci.*, *60*, 1733–1753.

Fu, X., B. Wang, and L. Tao (2006), Satellite data reveal the 3-D moisture structure of Tropical Intraseasonal Oscillation and its coupling with underlying ocean, *Geophys. Res. Lett.*, *33*, L03705, doi:10.1029/2005GL025074.

Fu, X., B. Wang, D. E. Waliser, and L. Tao (2007), Impact of atmosphere-ocean coupling on the predictability of monsoon intraseasonal oscillations, *J. Atmos. Sci.*, *64*, 157–174.

Fu, X., B. Yang, Q. Bao, and B. Wang (2008a), Sea surface temperature feedback extends the predictability of Tropical Intraseasonal Oscillation, *Mon. Weather Rev.*, *136*, 577–597.

Fu, X., B. Wang, Q. Bao, P. Liu, and B. Yang (2008b), Experimental dynamical forecast of an MJO event observed during TOGA-COARE period, *Atmos. Oceanic Sci. Lett.*, *1*, 24–28.

Hendon, H. H., B. Liebmann, M. Newmann, J. D. Glick, and J. E. Schemm (2000), Medium-range forecast errors associated with active episodes of the Madden-Julian Oscillation, *Mon. Weather Rev.*, *128*, 69–86.

Jiang, X., and D. E. Waliser (2008), Northward propagation of the subseasonal variability over the eastern Pacific warm pool, *Geophys. Res. Lett.*, *35*, L09814, doi:10.1029/2008GL033723.

Krishnamurti, T. N., M. Subramaniam, G. Daughenbaugh, D. Oosterhof, and J. H. Xue (1992), One-month forecast of wet and dry spells of the monsoon, *Mon. Weather Rev.*, *120*, 1191–1223.

Lin, J. L., et al. (2006), Tropical intraseasonal variability in 14 IPCC AR4 climate model. Part I: Convective signals, *J. Clim.*, *19*, 2665–2690.

Lorenz, E. N. (1993), *Chaos*, pp. 181–184, Univ. of Wash. Press, Seattle.

Maloney, E. D., and S. K. Esbensen (2003), The amplification of East Pacific Madden-Julian Oscillation convection and wind anomalies during June–November, *J. Clim.*, *16*, 3482–3497.

Maloney, E. D., and D. L. Hartmann (2000), Modulation of eastern North Pacific hurricanes by the Madden-Julian Oscillation, *J. Clim.*, *13*, 1451–1460.

Shinoda, T., H. H. Hendon, and J. Glick (1999), Intraseasonal surface fluxes in the tropical western Pacific and Indian Oceans from NCEP Reanalysis, *Mon. Weather Rev.*, *127*, 678–693.

Shukla, J. (1998), Predictability in the midst of chaos: A scientific basis for climate forecasting, *Science*, *282*, 728–731.

Tian, B. J., D. E. Waliser, E. J. Fetzer, B. H. Lambrigtsen, Y. L. Yung, and B. Wang (2006), Vertical moist thermodynamic structure and spatial-temporal evolution of the MJO in AIRS observations, *J. Atmos. Sci.*, *63*, 2462–2485.

Vitart, F., et al. (2007), Monthly forecast of the Madden-Julian Oscillation using a coupled GCM, *Mon. Weather Rev.*, *135*, 2700–2715.

Waliser, D. E., W. Stern, S. Schubert, and K. M. Lau (2003), Dynamic predictability of intraseasonal variability associated with the Asian summer monsoon, *Q. J. R. Meteorol. Soc.*, *129*, 2897–2925.

Wang, B., and X. Zhou (2008), Climate variability and predictability of rapid intensification in tropical cyclone in the western North Pacific, *Meteorol. Atmos. Phys.*, *52*, 1–16, doi:10.1087/s00703-006-0238-z.

Wang, B., P. Webster, K. Kikuchi, T. Yasunari, and Y. Qi (2006), Boreal summer quasi-monthly oscillation in the global tropics, *Clim. Dyn.*, *27*, 661–675.

Yasunari, T. (1979), Cloudiness fluctuations associated with the Northern Hemisphere summer monsoon, *J. Meteorol. Soc. Jpn.*, *57*, 227–242.

Q. Bao, LASG, Institute of Atmospheric Physics, Chinese Academy of Sciences, 40 Hua-Yan-Li, Bei Chen Xi Road, Beijing 100029, China.

X. Fu, J.-Y. Lee, P. Liu, and B. Wang, IPRC, SOEST, University of Hawaii at Manoa, 1680 East West Road, POST Building 409D, Honolulu, HI 96822, USA. (xfu@hawaii.edu)